ELSEVIER

Chemical Physics 281 (2002) 373–391

Chemical Physics

www.elsevier.com/locate/chemphys

A versatile experimental approach for understanding electron transport through organic materials

Maria A. Rampi [a,*], George M. Whitesides [b,*]

[a] *Dipartimento di Chimica, Centro di Fotochimica CNR, Universita' di Ferrara, 44100 Ferrara, Italy*
[b] *Department of Chemistry and Chemical Biology, Harvard University, 12 Oxford Street, Cambridge, MA 02138-9857, USA*

Received 10 October 2001

Abstract

This paper describes an experimentally simple method for assembling junctions with nanometer-scale, structured organic films positioned between two metal electrodes. These junctions comprise two metal electrodes that sandwich two self-assembled monolayers (SAMs) – that is, metal (mercury)–SAM//SAM–metal (mercury, gold or silver) junctions. The junctions are easy to assemble (because the mercury electrode is compliant) and they are compatible with SAMs incorporating organic groups having a range of structures. This paper describes three different variations on this type of Hg-based junction. The first junction, formed by two contacting mercury drops covered by the same type of SAM, is a prototype system that provided useful information on the structure and electrical properties of the Hg-based junctions. The second junction consists of a Hg drop covered by one SAM (Hg–SAM(1)) in contact with a second SAM supported on a silver film (Ag–SAM(2)) – that is, a Hg–SAM(1)//SAM(2)–Ag junction. This junction allowed systematic measurements of the current that flowed across SAM(2), as a function of structure (for example, using aliphatic or aromatic thiols of different length), and a common SAM(1) of hexadecane thiol. The current density follows the relation $I = I_0 e^{-\beta d_{Ag,Hg}}$, where $d_{Ag,Hg}$ is the distance between the electrodes, and β is the structure-dependent attenuation factor for the molecules making up SAM(2): β was 0.87 ± 0.1 Å^{-1} for alkanethiols, 0.61 ± 0.1 Å^{-1} for oligophenylene thiols, and 0.67 ± 0.1 Å^{-1} for benzylic derivatives of oligophenylene thiols, in general agreement with the values calculated by other approaches. The same type of junction, but using SAM(1) and SAM(2) carrying suitable chemical groups, X and Y, was used to measure the rate of electron transfer across different types of functional groups and bonds: van der Waal interactions, H bonds, and covalent bonds. The third type of junction, Hg–SAM//R//SAM–Hg, is an electrochemical junction that can (i) trap redox-active molecules (R) in the interfacial region between the SAMs, and (ii) control the potential of the electrodes with respect to the redox potential of R using an external reference electrode. This system shows *I–V* curves with steps that can be interpreted in terms of redox cycling mechanism.

1. Introduction

Electron transfer is: (i) the basis for a number of biological processes central to life, and (ii) a fundamental feature of many processes of techno-

* Corresponding authors. Tel.: +39-0532-291162; fax: +39-0532-420709; tel.: +1-617-495-9430; fax: +1-617-495-9857.
E-mail addresses: rmp@unife.it (M.A. Rampi), gwhitesides@gmwgroup.harvard.edu (G.M. Whitesides).

0301-0104/02/$ - see front matter
PII: S0301-0104(02)00445-7

logical importance. In the last 50 years, electron transfer processes have been studied extensively, both theoretically and experimentally [1].

Investigations of electron-transfer processes have largely focused on the rates of transfer in solution between donor and acceptor species, either as separated entities or as separate sites of larger molecules [1]. Examinations of rates of electron transfer between covalently linked donor and acceptor units through a molecular bridge in species of the structure D–B–A (D = donor, A = acceptor, B = molecular bridge) have underlined the importance of the structure of the bridge in facilitating electron transfer from D to A. As a colloquial way to emphasize this role, it has been customary to refer to the bridge as a "molecular wire", and to discuss its ability to "conduct" electrons. This usage may (or may not) be technically correct, but it is certainly misleading. It should be clear that these expressions, however intended, imply an analogy between pathways for electron transfer through organic molecules and electron conductance through metallic conductors that does not exist. The term "molecular wire" encourages description of electron transport through molecules in term of metallic ("Ohmic") conductivity. In fact, none of the molecular bridges studied to date show Ohmic behavior: electron transfer through "molecular wires" occurs by electron tunneling, and organic wires are "conducting" in the same sense that polyethylene is conducting. The "molecular wires" facilitate electron transport relative to *vacuum*, but are not similar to metals either in the magnitude of their conductivity or in the mechanism of this conduction.

Most of our present understanding of electron transfer is based on measurements made in solution, but the conclusions from these studies do not necessarily hold for the same molecules in other environments (e.g. in the solid state). In their pioneering work in 1971, Mann and Kuhn [2] contrasted electron-transfer studies in molecular systems in solution with electron transport in the solid state; this work, for the first time, measured currents through molecular monolayers sandwiched between metal electrodes.

The use of molecular properties to make electronic devices was first envisaged by Aviram and Ratner [3] in a theoretical paper in 1974. Because there were no technologies that could establish electrical contacts across individual molecules, experimental investigations of the fundamental processes involved in electron transfer through molecules have focused on liquid-phase systems [1]. More recently, the well-defined structures of SAMs on metal electrodes have made it possible to study electron transport by electrochemistry [4–13].

Only in the late 90s has the combination of nanotechnology [14], scanning probe microscopies [15], and methods to form electrically functional connections to metal surfaces [16] triggered the fabrication of metal–molecule(s)–metal junctions, and opened the door to experimental "molecular electronics". Different type of junctions have been used to sandwich molecules (several, a few, or individual molecules) between two metal surfaces, and to measure their electrical properties [17–56]. Junctions that include organic molecules of modest structural complexity [18,19,21,23,24,31,32,35,37,38,50,52] have showed properties that suggested that it may be possible to build devices that mimic the function of electronic components (conductors, transistors, rectifiers, logic gates).

Whether or not molecular species will be used in practical microelectronic devices is still a matter of discussion [57,58]. Certainly organic and organometallic molecules deserve consideration as components of devices, because their electronic structure can be tuned with great precision by synthesis, and because self-assembly provides, in principle, a route toward fabrication of functional systems. The use of molecular components has, for example, been claimed to be the best ultimate strategy to achieve high-density memories and molecular computers [59–61]. Regardless of whether such devices are ever fabricated, the information gained from studies of molecular electronics will certainly be useful in formulating the relationships between molecular structures and rates of electron transport at the nanometer scale.

Although informative *I–V* characteristics for specific junctions have been identified [17–56] and discussed [17–56,59,60], the factors influencing the electrical properties of metal–molecule(s)–metal junctions is still incomplete for at least five reasons: (i) The correct interpretation of the *I–V*

curves is still difficult: for example, the contributions of interfacial processes relative to electron transport through organic material in determining conductivities remain unclear. (ii) The identification of specific mechanisms of transport of electrons through organic matter is controversial, particularly when redox sites are present in the junction: it is clear that tunneling is the dominant mechanism in many cases, but the details even of tunneling are incompletely understood. (iii) There is no completely satisfactory theoretical method describing a junction, and no way to calculate the I–V behavior for a given molecule–metal junction [42,57]. (iv) The effects of the electrical fields on the energy levels of the molecule are matters of speculation [42,46,62]. (v) The contact between molecules and metal electrodes is poorly understood both electrically and structurally [44,63].

We believe that a substantial body of experimental data is needed to provide a foundation for research in molecular electronics. Ideally, collecting this information would start with screening the electrical behavior of a wide range of organic/organometallic molecules with different molecular and electronic structures, and searching for broad generalizations relating structure and rates of electron transport. To reach this goal, a crucial step is the development of suitable experimental systems with which to measure the electrical properties of organic molecules. Each of the large number of junctions reported in the literature has both advantages and limitations. We believe that junctions are needed that are stable, reproducible, easy to assemble and to use, and broadly compatible with a range of organic structures. Ideally it should be possible to fabricate these structures on different surfaces (metals, non-metallic conductors, and semiconductors), to measure electrical properties over a range of temperatures, and generate statistically large number of data.

2. Metal–molecule(s)–metal (MIM) junctions

The most widely used approach to the fabrication of junctions has two steps: (i) organizing a monolayer of organic molecules on a metal surface, (ii) fabricating a second metal junction on top of the monolayer, usually by evaporation. The undefined structure of this second metal-organic junction remains an important ambiguity: there is an intuition that reaction of hot, reactive metal atoms with organic molecules will damage (or induce reaction in) these molecules, but there is no structural information concerning these interfaces.

Kuhn assembled the first metal–insulator–metal junction (MIM) used to study the electrical properties of monolayer films by depositing evaporated metals (Pb, Ag, Al) on top of a Langmuir–Blodgett (LB) film supported on aluminum surfaces [2]. Several groups still use variants of this basic technique to study the electrical behavior of molecules incorporated into LB films or SAMs organized at metal surfaces [18,19,22,31,32,35,38,39,44,51], although nanofabrication now makes it possible to fabricate junctions incorporating a much smaller numbers of molecules than those examined by Kuhn. For example, by evaporating gold through a nanopore mask on top of a SAM, Reed et al. [39] was able to reduce the area of a junction to a value below 700 nm^2. (Using small areas reduces the number of defects present in the SAMs, and therefore reduces the probability of shorting.) Although these systems have demonstrated interesting functionality, there are two experimental difficulties that complicate the interpretation of the data they generate: (i) The nature of the interface formed by the evaporation of metal atoms onto the organic films is totally undefined. (ii) Electrical shorts, perhaps due to percolation of Au atoms into the organic molecules, (or defects or damage to the SAMs), have limited their reproducibility.

Scanning probe microscopies (SPM) have been increasingly used to measure current flowing across molecular systems organized at a gold surface [20,23,24,30,33,36,37,41,42,46,47,52,54,55]. SPM-based methods have made it practical to study electron transport through single molecules or small collection of molecules. In many cases, however, the interpretation of the results of STM experiments is complicated by the convolution of the tip-substrate distance with the conductance. Conducting-probe AFM (CP-AFM) obviates this problem by controlling the position of the metal-coated tip with respect to the substrate using force

feedback. Recent work by Wold and Frisbie [30,33] and Lindsay et al. [24] have demonstrated that tunneling current can be accurately measured by CP-AFM.

Others, less conventional junctions have also been assembled. The most creatively designed, and probably the most difficult to reproduce, are the "break junctions" [40,51] first explored for this purpose by Reed [52]; in this system, the two tips of a broken metal wire sandwich molecule(s) of a dithiol. Other junctions have used strong electrical fields to fish long molecules (>100 Å) from dilute solutions across electrodes situated a few nanometer apart [53]. A new type of junction have been recently assembled by cross-contacting two thin (10 μm) gold wires covered by SAMs [17]. We [26–29,45,48] and Majda [34,43] have developed MIM junctions based on drops of liquid Hg as electrodes.

3. Results and discussion

3.1. MIM junctions based Hg electrode(s)

We have assembled, characterized, and studied different types of junctions, all using Hg-based electrodes: Fig. 1 sketches these junctions; they are (i) easy to assemble (their assemble does not require sophisticated, expensive apparatus); (ii) stable and reproducible (only 20% of the junctions short or show anomalous conductivity); (iii) versatile (they can host a large variety of molecules and molecular systems). Drops of Hg as electrodes provide four advantages: (i) The Hg surface, as a liquid, is free of structural features – edges, steps, terraces, pits – that result in defects of the adsorbed monolayer. (ii) Hg forms well-ordered SAMs after contact with alkanethiol-containing solutions for only a few seconds [8,64–67]. (iii) The Hg drop conforms to the topography of solid surfaces, and forms a good conformal contact with molecular monolayers on a solid surface. (iv) The Hg drops form alkanethiolate SAMs that show liquid-like behaviors [8] (a SAM-covered drop of Hg is therefore able to conform to a solid surface without cracking the SAM). In addition, when the junction consists of a solid metal and a mercury electrode, each supporting a SAM, the chemical composition of the two SAMs can be different, and a variety of different metals can be used in the solid electrode [45].

3.1.1. Nomenclature

We will describe the junctions using the nomenclature: $J_{Hg\text{–}SAM//SAM\text{–}M}$, where // represents the interface between the SAMs, M the metal of the surfaces (Au, Ag, Hg), and – is the interface between the thiol group and the metal. We have assembled and studied: (a) junctions with two Hg electrodes, $J_{Hg\text{–}SAM//SAM\text{–}Hg}$ (Fig. 1(a)); (b) junctions with one Hg and one solid metal electrode, $J_{Hg\text{–}SAM(1)//SAM(2)\text{–}M}$ (Fig. 1(b)) and (c) junctions where redox sites, R, are trapped at the interface between the SAMs and are in electrical contact with a distant reference electrode via an electrolyte solution, $J_{Hg\text{–}SAM//R//SAM\text{–}Hg}$, (Fig. 1(c)). Fig. 2 sketches the interfaces of these junctions and the molecular systems organized at the electrodes.

3.1.2. The mercury–mercury junction, $J_{Hg\text{–}SAM//SAM\text{–}Hg}$

This junction is formed by bringing two drops of Hg covered by SAMs into contact in a solution of ethanol containing alkanethiol inside a microsyringe.Two tungsten wires are inserted into the Hg drops as electrodes: one electrode is inserted in the upper drop; its position is marked in Fig. 1(a). The second electrode, not shown in Fig. 1, is inserted in the lowest Hg drop through the syringe needle. Fig. 1(a) shows both a single junction and three junctions in series and the relative capacitance values for SAMs formed by hexadecanethiol. Using capacitance measurements as a function of length of the alkanethiols forming the SAMs, and impedence spectroscopy, we have characterized the equivalent circuit of the junction, and established a high resistivity for the alkanethiolate SAMs ($\sigma = 6 \times 10^{-15}\ \Omega^{-1}\ \mathrm{cm}^{-1}$) [48]. Capacitance measurements in polar solvents (ethanol, water) indicated that the junction formed with hexadecane thiol (i.e., a SAM with a hydrophobic surface) does not include significant amounts of these solvents between the two SAMs (see Fig. 2(a)) [48]. Capacitance values using this junction in hydrocarbon solvents (hexadecane, octane, heptane) are 10 times smaller than

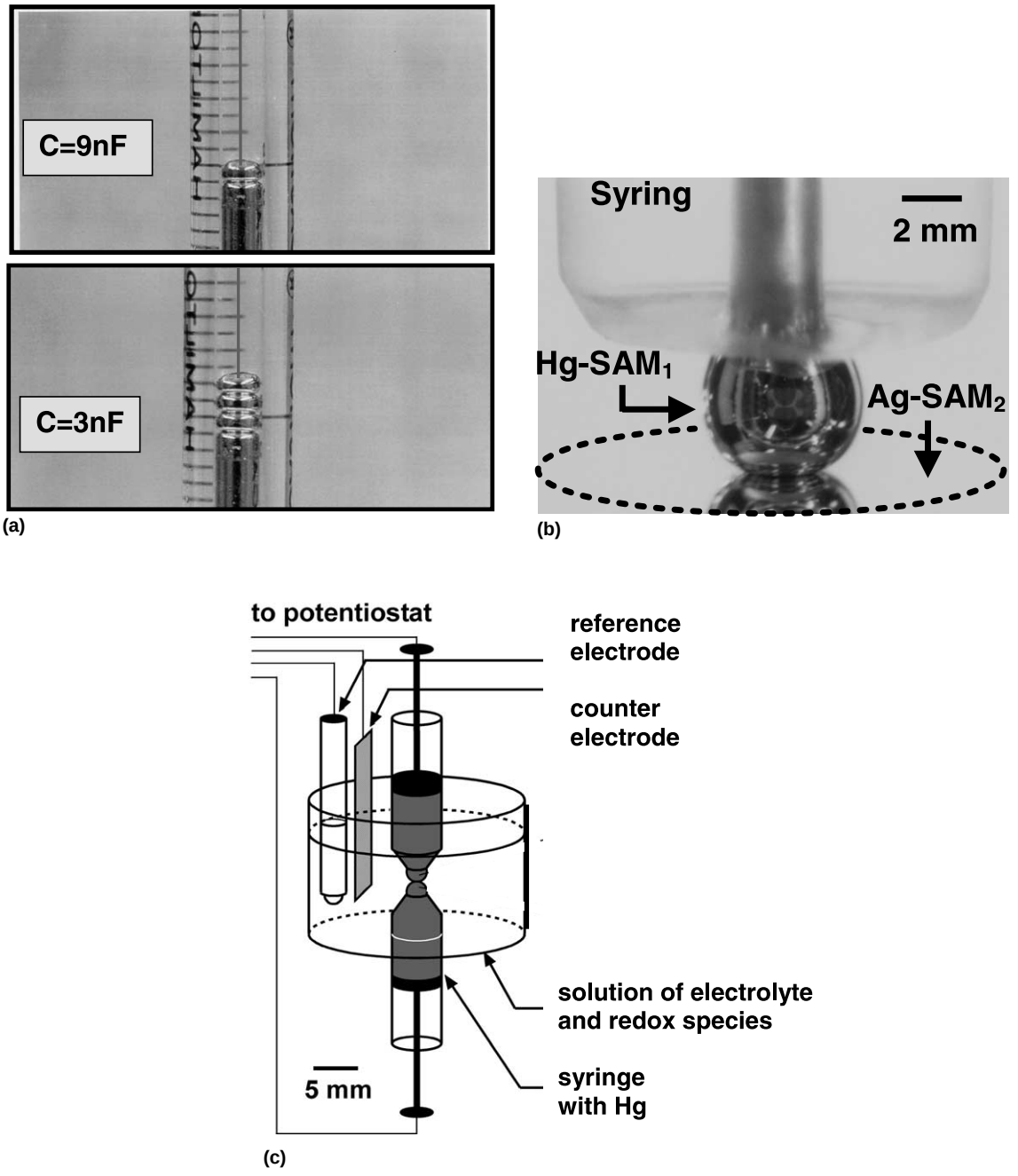

Fig. 1. The Hg based junctions: (a) Photographic images of the $J_{Hg\text{–}SAM//SAM\text{–}Hg}$ forming one capacitor and three capacitors in series: one electrode is inserted into the top Hg drop (in the position marked on the image as a dark vertical line) and the second (not shown) is inserted in the lower drop, through the syringe needle (from [48]). (b) Photographic image of $J_{Hg\text{–}SAM(1)//SAM(2)\text{–}Ag}$ (from [28,29]). (c) Schematic view of $J_{Hg\text{–}SAM//R//SAM\text{–}Hg}$.

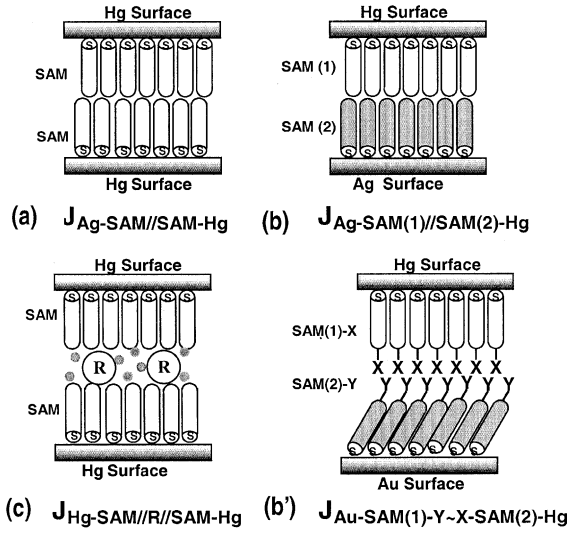

Fig. 2. Schematic representation of the interfaces of the Hg-based junctions: (a) the "liquid–liquid" junction $J_{Hg\text{–}SAM//SAM\text{–}Hg}$. (b) The "liquid–solid" junction $J_{Hg\text{–}SAM(1)//SAM(2)\text{–}Ag}$. (b′) The "liquid–solid" junction $J_{Hg\text{–}SAM(1)\text{–}Y\sim X\text{–}SAM(2)}$ (b and b′ have the geometry represented in Fig. 1(b), but different interfaces). (c) The "inclusion" junction $J_{Hg\text{–}SAM//R//SAM\text{–}Hg}$.

expected assuming a dielectric constant of $\varepsilon \sim 2.5$; these values suggest that some solvent is included at the interface under these conditions across this junction (when no voltage is applied). When a voltage *is* applied across this junction, experimental results (see Sections 3.1.3 and 3.2.1) imply that solvent is not included; thus the presence or absence of hydrocarbon solvents between hydrocarbon SAMs may depend on the pressure (reflecting the applied electrical potential) across the junction.

In general, the quantity and influence of the solvent at the interface between SAMs in these junctions are still incompletely defined. The behavior of solvents confined in subnanometer films is, of course, a subject of general inquiry [68]: experiments [69] and simulations [70] have shown that both water and organic solvents undergo layering and phase transition near smooth, solid, surfaces, each solvent at a different distance from the solid surfaces.

The " mercury–mercury" junction has the advantage that it uses the same metal (Hg) for the two electrodes, and thus avoids any issue of contamination of the metal used in a solid electrode by mercury through vapor transport. This junction also has several disadvantages: (i) It is difficult to evaluate the contact area. (ii) At high voltages, the facing SAMs may alter their structure by intercalation, compression, spreading, or some other mechanism, as Majda and Slowinski pointed out [34]. (iii) The junction cannot be used with certain types of SAMs (for example, those generated by polyphenylene-derived thiols).

3.1.3. The liquid–solid junction, $J_{Hg\text{–}SAM(1)//SAM(2)\text{–}M}$

This junction is formed by using a Hg drop covered by a SAM, and a solid metal surface (M = Au, Ag, Cu, Hg, Pd, Hg/Au alloy) covered by a second SAM (Fig. 1(b)). The fabrication of these junctions is straightforward: in all cases, the SAMs are formed separately on the Hg drop and on the solid metal surface. The two metal surfaces covered by SAMs are brought in contact by the use of a micromanipulator in a solution (usually hexadecane) containing the thiol (hexadecanethiol) used to make the SAM on Hg. The presence of this liquid phase (i) protects the mercury drop from vibration, (ii) patches defects created when the SAM covering the Hg drop contacts the solid surface and (iii) protects the surface of the SAMs from atmospheric contamination. When a liquid–solid junction incorporating hydrophobic SAMs is assembled in different hydrocarbon solvents (isooctane, hexane, toluene, hexadecane), similar current densities are measured across the junction (Fig. 3); this observation suggests that solvent is not trapped at the contact areas. Results (see Section 3.2.1, Fig. 7(b)) strongly support this conclusion.

The ease with which the "liquid–liquid" junction is assembled makes it possible to perform a number of measurements on the same sample: after each measurement, the syringe used to form the mercury drop is lifted, and the contact of the drop with the surface broken. The solid, planar, electrode is then translated laterally by about 1 mm and the drop of mercury again brought into contact with the surface. (This procedure, carried out in a solution of hexadecanethiol in hexadecane, allows possible damages to the SAMs on Hg to heal between two measurements.) The cycle of

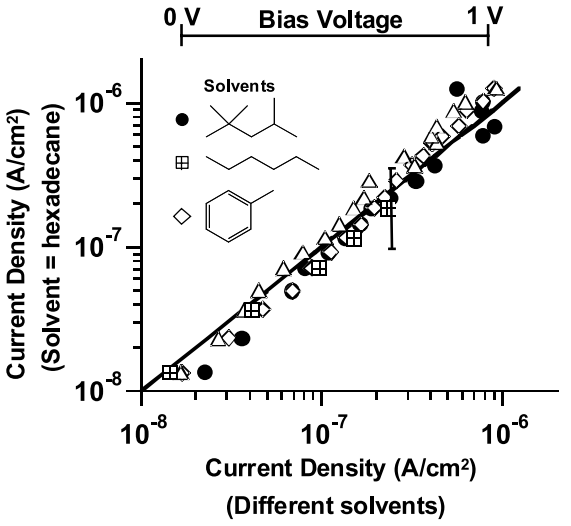

Fig. 3. Plot of average current density (from 0 to 1 V) for a junction with structure $J_{Hg-C_{16}//C_{10}-Ag}$ formed using hexadecane as solvent, against current density (from 0 to 1 V) for junctions with the same structure but using iso-octane, *n*-hexane, or toluene as solvent. The symbols are defined on the plot. △ represent values of current density for a junction where SAM(2) is formed from $CH_3(CH_2)_9SH$ and $[CH_3(CH_2)_9S]_2$ in 1:1 molar ratio. The solid line is that expected when the current density on the *y*-axis equals that on the *x*-axis.

assembly, measurement, and disassembly can be repeated as many time as the area of the solid surfaces allows it. It is thus easy to make statistically significant number of measurements. The areas of each junction were estimated visually by magnification of the contact at 40× magnification.

The SAM on Hg (SAM(1)) and on the solid surface (SAM(2)) can be formed by molecules of different structures (Figs. 2(b) and (b′)). The use of a solid surface increases the versatility of the junction substantially, relatively to the liquid–liquid junction: (i) On a solid surface it is easy to characterize the organization of the molecules forming the SAM. (ii) The organization of the same molecules can be changed by changing the metal substrate: for example, saturated [71] and conjugated [72] chains form SAMs having different tilt angles on Ag and Au films. (iii) The contact area can be evaluated easily. (iv) A large range of organic structures can be included in the SAM(2) on the solid surface, and the organization and the structure of these SAMs can be characterized. We have demonstrated that this junction can sustain high electrical fields (6 MV cm^{-1}) without electrical breakdown for SAM(2) formed by molecules with very different structures (alkanes, polyphenylene, derivatives of anthracene and cholesterol) and on the different metals (Ag, Au, Hg, Au/Hg alloy) [45].

3.1.4. The inclusion junction, $J_{Hg-SAM//R//SAM-Hg}$

In this junction (Fig. 1(c)), R is a redox molecule trapped at the interface between the two SAMs, (Fig. 2(c)).

Two-electrode systems suffer from an ambiguity in the relative positions of the Fermi levels of the electrodes with respect to the energy levels of the redox molecules sandwiched between them. In the electrochemical cell represented in Fig. 1(c), the junction is immersed in an electrolyte solution, and a macroscopic reference electrode allows potentiostatic control of the energy levels of redox sites trapped in the junction, relative to the potentials applied to the metal electrodes. We believe that a layer of electrolyte (represented schematically by Fig. 2(c)) is present at the interface (in this case the SAMs are formed by thiols carrying hydrophilic groups (–COOH)), and that this layer is responsible for the electrical contact between the reference and working electrodes and the redox species. It is, however, difficult to infer details of the nature, the thickness, and the structure of this layer [68–70]. The electrical neutrality of the solution is provided by lateral movements of ions in the thin electrolyte film (Fig. 4). The SAMs form inert spacers between the mercury electrodes and the layer of electrolyte containing the redox molecules: this spacer permits electron transfer between the electrodes and the redox molecules by tunneling.

We use this review to summarize the results obtained using these Hg-based junctions. We have used $J_{Hg-SAM//SAM-Hg}$ (Figs. 1(a) and 2(a) as a prototype to characterize the equivalent circuit of the junction; the complexities pointed by Majda and Slowinski [34] can cloud interpretation of the results from this system. We have used $J_{Hg-SAM(1)//SAM(2)-M}$ (M = Ag, Au) (Fig. 1(b)) to correlate electrical properties of the junction with the chemical structure of the molecules

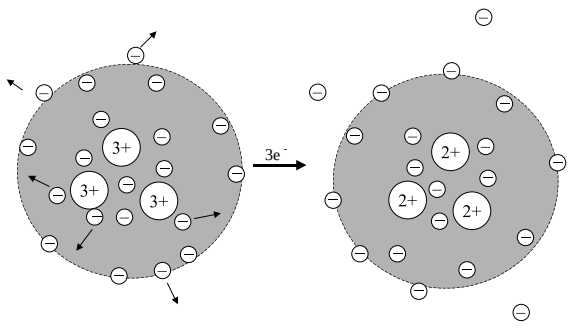

Fig. 4. Schematic representation of lateral movements of electrolyte ions in the thin, interfacial layer of electrolyte in $J_{Hg\text{–}SAM//R//SAM\text{–}Hg}$; this movement allows the interfacial layer to be electrically neutral overall, and allows the redox molecules in the layer to be in thermodynamic contact with the bulk solution and the reference electrode.

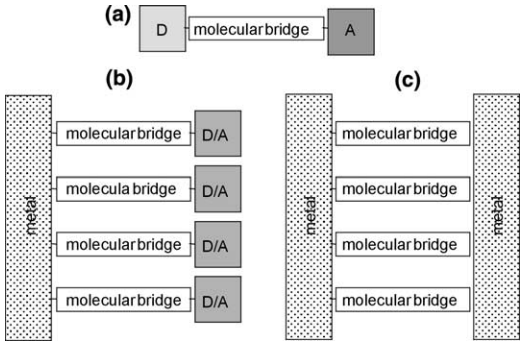

Fig. 5. (a) sketches a D–B–A system. The processes of electron transfer from the donor (D) to the acceptor (A) site across the molecular bridge (B) can be monitored in solution by time-resolved photophysical techniques. (b) This figure sketches an electroactive SAM on a metal surface. This system is made of a molecular bridge (B), appropriately anchored to the metal surface, terminating with an electroactive group (D/A). In such an arrangement, the use of fast electrochemical techniques can lead to the determination of heterogeneous electron-transfer rates from/to the metal surface to/from the electroactive group across the molecular wire. (c) Represents a metal–SAM–metal junction schematically; in this system, an array of molecules bridges two metal surfaces. In this type of experimental arrangement, the rates of electron transfer are measured as current density as a function of applied potential.

forming the SAMs (Fig. 2(b), (b′)). The junction $J_{Hg\text{–}SAM//R//SAM\text{–}Hg}$ has made it possible to control the potential of the electrodes with respect to that of the redox sites in tunneling contact with the electrodes (Fig. 2(c)), and to demonstrate the behavior of redox sites confined in a nanometer gap.

3.2. Correlation between electrical properties and chemical structure

An approach to understanding the mechanism of electron transfer through organic matter is to correlate the rates of electron transfer with the molecular structure of the matter through which the electrons move. We have measured and compared rates of electron transfer through molecules of different structures organized in SAM(2) on Ag surfaces of a junction of structure Hg–SAM(1)// SAM(2)–Ag.

Fig. 5 summarizes different experimental approaches used to measure and compare electron-transfer rates. The most extensively used experimental approach for chemists are those that have examined the rates of electron transfer using molecular systems in solution (D–B–A systems), where the donor (D) and acceptor (A) are covalently linked through a molecular bridge (B) (Fig. 5(a)) [73–75]. The extensive literature [73–75] describing these systems indicates that the rate of electron transfer (k_{et}) depends exponentially on the distance between D and A according to Eq. (1), where k_{et} is the electron-transfer rate, d is the length of the bridge, and β is the so-called "decay factor" that correlates the rate of electron transfer with the chemical structure of the bridge. Table 1 lists values of β that have been reported for D–B–A structures in which

$$k_{et} = k_0 e^{-\beta d} \tag{1}$$

the bridge was based on saturated hydrocarbons [73,76,77], and polyphenylenes [75,78,79]. Using the same approach, electron transfer has also been studied in biological systems. Rates of electron transfer between different proteins [80–82] and through DNA [83–85] have been measured by several groups. This approach measures β accurately, but requires (i) a rigid conformation of the bridge in solution, and (ii) a substantial synthetic effort.

SAMs on metal surfaces provide a different approach to the measurements of rates of electron transfer as a function of distance (Fig. 5(b)) [4–13]. SAMs of organic thiols on the surface of a metal

Table 1
Values of β (Å^{-1}) for aliphatic and oligophenylene chains obtained with different experimental systems

System	Aliphatic chains	Polyphenylenes chains	Comments
D–B–A molecular systems	0.8–1 [73,76,77]	0.4–0.6 [75,78,79]	Transient spectroscopy provides accurate measurements of electron-transfer rate. The values are affected by uncertainties in the distance between donor and acceptor
Electrochemical approach	0.9–1.2[a] [8–13]	–	The large tilt angle of aliphatics SAMs on Au (30°) allows for a contribution of a through space mechanism to the electron transfer process
MIM junctions	1.4[d] [2], 0.89[c] [41], 0.99[a] [17], 0.87[b] [this work]	0.6[b] [this work]	The highest value for aliphatic chains is probably influenced by the presence of layers of Al_2O_3 on the electrodes
STM	1.2[a] [47]	–	STM is still a difficult approach for quantitative, comparable measurements
AFM	1.1[a] [33], 0.94[a] [this work]	0.47[a] [this work]	The general agreement of the values obtained by the AFM and the Hg-based junctions with those using D–B–A systems is the most interesting result (see Discussion)

[a] Monolayers formed on Au.
[b] Monolayers formed on Ag.
[c] Monolayers formed on Hg.
[d] Monolayers (LB films) formed on Al.

electrode (Ag, Au, and Hg) are thin films with thicknesses that are well defined and that can be changed by varying the length of the organic groups [16,71]. A redox active center tethered to the SAMs can be separated from the surface of the electrode by increasing distances using organic synthesis and self-assembly. Rates of electron transfer measured by this approach also follow the relation in Eq. (1). Values of β determined by this approach have been reported for alkanethiols [8–13], and for phenylene–ethynylene oligomers [6,7] and other conjugated molecules [4,5].

A third approach to measuring electron transport, which is more familiar to physicists than to chemists, uses junctions (Fig. 5(c)). The work of Mann and Kuhn [2] started these studies – studies in which current densities were measured as a function of the thickness of organic layers sandwiched between the electrodes of a junction – and others have continued it. Majda et al. [43] and Weiss et al. [47] also determined the correlation parameter β for aliphatic chains using alkanethiol SAMs of different thickness. More recently, Wold and Frisbie [33] used a CP-AFM apparatus to measure current as function of the length of aliphatic chain.

Table 1 reports values of β for alkane and polyphenylene chains, measured using the different approaches depicted in Fig. 5.

We have compared rates of electron transfer through saturated and unsaturated molecules of different length by measurements of current density, and determined values of β (i) using junctions of the type $J_{\text{Hg–SAM(1)//SAM(2)–Ag}}$ [28,29], and (ii) (in collaboration with Frisbie) using a CP-AFM [86].

3.2.1. The values of β from junctions $J_{Hg–SAM(1)//SAM(2)–Ag}$

These junctions provide data that can be used to compare electron-transfer rates through different molecules forming the SAMs. To calculate β, we have used a strategy in which we have maintained the structure of SAM(1) constant, and varied the structure and the thickness of SAM(2) (Fig. 2(b)). The presence of SAM(1) on Hg is necessary for the mechanical and electrical stability of the junction, and does not affect how the current depends on the thickness of SAM(2). We have assembled three series of junctions, where SAM(2) was formed from alkanethiols, $HS(CH_2)_{n-1}CH_3$ ($n = 8, 10, 12, 14, 16$), oligophenylene thiols, $HS(Ph)_kH$ ($k = 1, 2, 3$), and benzylic

homologs of the oligophenylene thiols $HSCH_2(Ph)_mH$ ($m = 1, 2, 3$). In each junction, SAM(1) was formed from hexadecanethiol. Fig. 6 shows the current densities across these junctions as a function of applied voltage. The *I–V* curves of Fig. 6 indicate that: (i) the *shapes* of the *I–V* curves are the same for C_n, Ph_kH, and CH_2Ph_mH; (ii) the magnitudes of the current densities decrease in the order $Ph_kH > CH_2Ph_mH > C_n$ for films of the same thickness; (iii) the magnitudes of the current densities depend on the thickness of the monolayers. The decrease in current density with increasing length of the molecules forming SAM(2), and therefore with the distance separating the electrodes ($d_{Ag,Hg}$), followed the relation $I = I_0e^{-\beta d_{Ag,Hg}}$ as expected for tunneling (Fig. 7(a)). For alkanethiols forming SAM(1) on Ag, $\beta = 0.87 \pm 0.1$ Å^{-1}; for oligophenylene thiols, $\beta = 0.61 \pm 0.1$ Å^{-1}; and for the benzylic derivatives of oligophenylene thiols, $\beta = 0.67 \pm 0.1$ Å^{-1}. The values of β are approximately independent of V (over the range 0.1–1 V).

These values of β are in good agreement with corresponding values obtained by photoinduced electron transfer in molecular D–B–A systems [73,75–79] (see Table 1), and by electron transfer between a solid electrode and redox-active species in solution [8–13]. In D–B–A systems, values of β for aliphatic chains range from 0.8 to 1.0 Å^{-1} [73,76,77], and for polyphenylene chains range from 0.4 to 0.6 Å^{-1} [75,78,79]. In electrochemical approach β ranges from 0.9 to 1.2 Å^{-1} for alkane

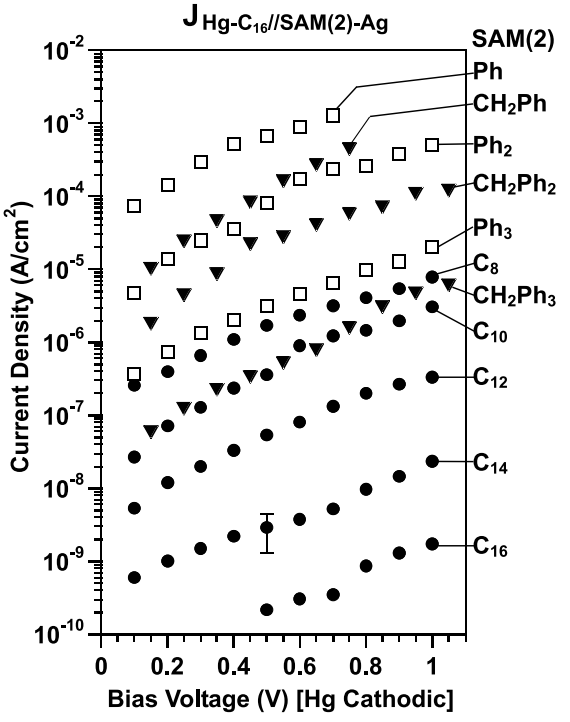

Fig. 6. Plots of current density as a function of the bias voltage between the mercury and silver electrodes for $J_{Hg-C_{16}//SAM(2)-Ag}$ junctions. The symbols used to represent different classes of compounds forming SAM(2) are: (●) $HS(CH_2)_{n-1}CH_3$; (□) $HS(Ph)_kH$; (▼) $HSCH_2(Ph)_mH$. The length of the error bar is representative of the standard deviation, from data obtained using statistically significant populations ($N = 20$) of junctions (from [28,29]).

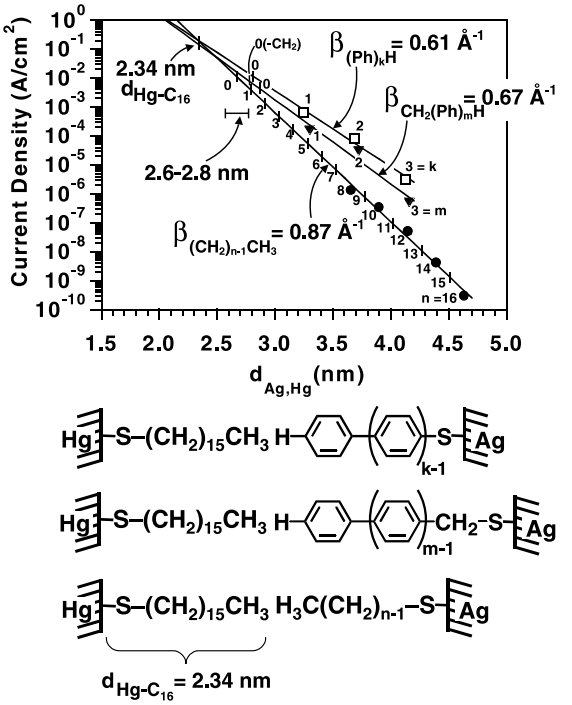

Fig. 7. (a) Plot comparing the distance dependence of current density in $J_{Hg-C_{16}//SAM(2)-Ag}$ for SAMs composed of aliphatic thiols $HS(CH_2)_{n-1}CH_3$ (●); oligophenylene thiols $HS(Ph)_kH$ (□); benzylic homologs $HSCH_2(Ph)_mH$ (▼). Current density were obtained at 0.5 V bias. The error in β is ~ 0.1 Å^{-1}. (b) Schematic representation of junctions formed from the three classes of thiols (from [28,29]).

chains, and from 0.36 to 0.57 Å^{-1} for polyphenylene–ethynylene chains [6,7]. The agreement among the values of β in these solid-state junctions, in molecular systems in solution, and across SAMs on solid electrodes suggests that all three types of processes involve tunneling as a common mechanism. A new type of junction [17], based on crossed gold wires that support SAMs, shows values of β for aliphatic and conjugated molecules in general agreement with our results.

Fig. 7(a)) shows the crossing point of the extrapolated plots of current density against $d_{\text{Ag,Hg}}$ for the three sets of junctions, $J_{\text{Hg–C}_{16}//\text{CH}_3(\text{CH}_2)_{n-1}\text{S–Ag}}$, $J_{\text{Hg–C}_{16}//(\text{Ph})_k\text{–Ag}}$, and $J_{\text{Hg–C}_{16}//(\text{Ph})_m\text{CH}_2\text{–Ag}}$. At the intersection point, in principle, there is no contribution to the junctions from an organic monolayer on silver. The thickness calculated for the hypothetical junction $J_{\text{Hg–C}_{16}//\text{Ag}}$ (where there is no hydrocarbon layer on silver) is $d_{\text{Ag,Hg}} = 2.34$ nm (Fig. 7(b)); we estimated that the thickness, for a junction in which the organic groups on silver had been removed, and only the Ag–S bond and the van der Waals radius of the terminal methyl group or hydrogen atom remain, is $d_{\text{Ag,Hg}} = 2.6$–2.8 nm. The difference between 2.34 and 2.6–2.8 nm – 0.3–0.5 nm – is a reasonable value for an aggregated contribution to the thickness from the Ag–S bond, the S–C bond, and the van der Waals radii of the terminal groups. These values suggest that there is no film of solvent trapped between the SAMs in the contact area of the junction. The consistency of the intersection values of the extrapolated plot for the three sets of organic compounds suggests that they are directly comparable.

3.2.2. Theoretical model

To fit the *I–V* curves, we, in collaboration with Mujica and Ratner, used a theoretical model that considers the structure of the tunneling barrier to be formed by molecules, rather than a homogeneous, unstructured medium [87]. This model considers off-resonance tunneling of electrons across a single molecule in a metal–molecule–metal junction in response to the applied voltage. The model assumes that (i) the molecules in the monolayer act independently (i.e., the total current density is the product of the molecular current times the molecular density), and (ii) the electrostatic potential profile is determined self-consistently through the combined solution of Poisson and Schrödinger equations [88]. According to this model, the electrostatic potential is approximately constant in the region of the molecular bridge, and drops at the electrode–molecule interfaces.This model gives Eq. (2), where n is the number of molecules per unit area, N is the number of "sites" that compose a homogeneous molecular bridge, t is the transfer integral between sites, Δ_0 is the spectral density of either of the two electrodes at zero bias, and ϕ is the difference between the Fermi level of the electrode and the energy of each site. A "site" in this model is an atom or a group of atoms whose orbital overlap provides the best superexchange pathway for electron transfer along a one-dimensional path [89]. Eq. (2) predicts (i) an exponential dependence of the current on the length of the

$$I(V) = \frac{2e}{\pi\hbar}\frac{\Delta_0^2}{(1-2N)t}n\left\{\left(\frac{e\phi + (eV/2)}{t}\right)^{1-2N} - \left(\frac{e\phi - (eV/2)}{t}\right)^{1-2N}\right\}, \tag{2}$$

$$\beta = \frac{2}{a}\ln\left(\frac{e\phi - (eV/2)}{|t|}\right) \tag{3}$$

molecule (L) since $I \propto \mathrm{e}^{-\beta L}$ (β, derived from Eq. (2), is given by Eq. (3), for positive bias, $\phi < eV/2$, and a the distance between two sites), and (ii) a weak dependence of β on V.

When Eq. (2) is fitted to the experimental *I–V* curve for $J_{\text{Hg–C}_{16}//\text{C}_{10}\text{–Ag}}$ ($d_{\text{Ag,Hg}} = 39$ Å), using ϕ, a, N, and t as floating parameters, we obtain $\phi = 4.6$ V and $t = -1.2$ eV, for $N = 15$ and $a = 3$ Å (Fig. 8): these values have a physically plausible interpretation [90,91]. Using these values in Eq. (3), we obtain a value of $\beta = 0.9$ Å^{-1} that is approximately constant over the range 0–1 V. This prediction of a weak dependence of β on the applied voltage is compatible with our experimental observations. The calculated product of N and a is close to the interelectrode separation (39 Å). The values of N and a do not correspond directly with simple picture of the "conductive pathway", but

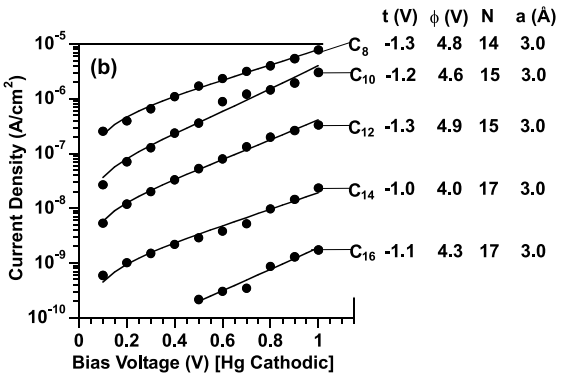

Fig. 8. Plot of the current density as a function of the bias voltage for junctions with composition $J_{Hg-C_{16}//C_n-Ag}$ ($n = 8, 10, 12, 14, 16$). The solid line represents the best nonlinear, least-squares fits of the data for each junction to Eq. (2). Each line in the figure is a fit to Eq. (2) using four floating parameters (see text) (from [29]).

do lead to a hypothesis that this path might involve *every other* CH_2 group in a polymethylene chain [92].

We observe that the experimental data fit Eq. (2) well, particularly given the assumption that the total current is simply the product of the current/molecule by the number of molecules per cm^2 (estimated to be $\sim 5 \times 10^{14}$) [29].

3.2.3. The values of β from CP-AFM

We have collaborated with Frisbie et al. [86] in investigating electron transport through SAMs composed of either alkanethiolates or oligophenylene thiolates of different length, using as a junction a conductive probe atomic force microscope (CP-AFM). The current–voltage characteristics of both types of SAMs were linear over ±0.3 V, and the current measured follow Eq. (1). The plot of the measured resistance as a function of the molecular length gives $\beta = 0.47\ \text{Å}^{-1}$ for the oligophenylene thiolate, and $\beta = 0.94\ \text{Å}^{-1}$ for the alkanethiolates. The values, reported in Table 1, show (i) the expected difference in the β values for these compounds (ii) agreement with those found using $J_{Hg-SAM(1)//SAM(2)-M}$. These results also show that CP-AFM is a reliable method for fundamental studies of electron transfer through a small number of organic molecules.

3.2.4. Comparison of electron transfer rates through different types of bonds and non-bonding interactions

The procedure with which the "liquid–solid" junction, $J_{Hg-SAM(1)//SAM(2)-M}$, is assembled makes it straightforward to use a SAM(1) and a SAM(2) that terminate in different functional groups (X and Y), and to compare rates of electron transfer through different types of molecular interactions between X and Y (Fig. 2(b′)).

Rates of electron transfer across groups connected by van der Waals interactions and hydrogen or ionic bonds may be important in determining the rates of electron transfer across proteins [93]. In proteins, a physical "tunneling pathway" for electron transfer is defined by a combination of interacting bonds and atoms that link donor with acceptor, and the electron transfer rate [94]. It is challenging to compare electron-transfer rates through different types of interactions [95] because comparisons required the use of model molecular systems where the same donor and acceptor groups are connected by different type of interactions [8,95–97]. We used a junction J_{Hg}–SAM(1)–X ∼ Y–SAM(2)–Au, where the solid surface was Au and where ∼ represents the interaction between X and Y, to compare electron transfer rates across covalent bonds and non-covalent interactions.

To study non-covalent interactions, we used X = –COOH, $–CH_3$, $–NH_2$ and Y = –COOH, $–CH_3$. It was also possible to bridge two SAMs covalently by reaction of a SAM on gold terminated with anhydride groups with a second SAM on mercury terminated in amine groups. It has been reported that this reaction generates a 1:1 mixture of two kinds of bridging groups: a covalent amide –C(O)–NH– group and a hydrogen-bonded $–CO_2H \cdots NH_2–$ pair (⋯ represents the notation for a H bonded interaction) [98]. Fig. 9 shows the current density measured under an applied voltage for these junctions, and demonstrates that it depended significantly on the structure of the interface. If the junction having only van der Waals interactions at the interface is used for comparison, the increase of the electron-transfer rate for the other interaction is calculated as

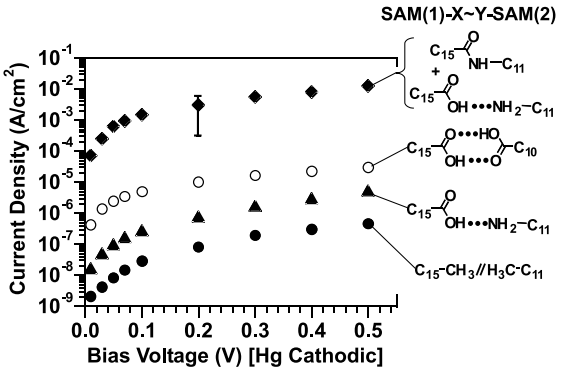

Fig. 9. Plots of the current density as a function of the bias voltage for $J_{Hg\text{–}SAM(1)\text{–}X\sim Y\text{–}SAM(2)\text{–}Au}$. The error bar is ± the standard deviation of the data (from [29]).

$$I_{(\text{–}CO_2H\cdots NH_2\text{–})}/I_{(\text{–}CH_3//H_3C\text{–})} \approx 9,$$

$$I_{(\text{–}CO_2H\cdots HO_2C\text{–})}/I_{(\text{–}CH_3//H_3C\text{–})} \approx 40,$$

and

$$I_{(\text{–}C(O)NH\text{–}/\text{–}CO_2H\cdots NH_2\text{–})}/I_{(\text{–}CH_3//H_3C\text{–})} \approx 10^4$$

(this difference becomes $\sim 10^3$ after correcting for small differences in the thickness of the organic films) [97]. The difference in current across an interface having only van der Waals interactions and an interface containing covalent bonds is equivalent to approximately six sigma bonds. Majda et al. [8] obtained similar results comparing electron-transfer rates along the chains (through-bond) and through adjacent chains (through-space) in alkanetiolate SAMs. The increase of the electron transfer rate we observe across $\text{–}CO_2H\cdots NH_2\text{–}$ and $\text{–}CO_2H\cdots HO_2C\text{–}$ bridges is similar to those reported by Nocera et al. [96] in model systems. The theoretical models developed by Beratan and Onuchic [94] to fit experimentally determined rates of electron transfer in proteins suggest that rates of electron transfer through these bonds should scale in the following orders: covalent>non-covalent bonds, and hydrogen bonds>van der Waals contacts. We observe these trends in the experimental results. The results obtained using these junctions are in good agreements with the limited experimental [8,96,97] and theoretical data [94,99]; they indicate that these systems will provide a useful approach to measurements of electron-transfer rates across other, different, kinds of interactions.

We note that, although these results seem internally consistent, there remain ambiguities concerning the extent to which solvent might be associated with or incorporated into the interface between the SAMs.

4. Redox sites confined inside a junction

"Inclusion junctions", $J_{Hg\text{–}SAM/R/SAM\text{–}Hg}$, (Figs. 1(c) and 2(c)) allow redox species (R) to be sandwiched between the Hg–SAM interface and the potential applied to the two Hg electrodes to be controlled with respect to the potential of R. We assembled two junctions: junction $J_{Hg\text{–}SAM//Ru(III)//SAM\text{–}Hg}$ (where $Ru(III) = Ru(NH_3)_6Cl_3$, with a bulk concentration of 1 mM in 0.1 M NaF in water, and the SAMs are formed from mercaptoesadecanoic acid), and $J_{Hg\text{–}SAM//TCNQ//SAM\text{–}Hg}$ (where TCNQ = 7,7,8,8-tetracyanoquinodimethane, with a bulk concentration of 1 mM in 0.1 M tetrabutylammonium hexafluorophosphate in acetonitrile, and the SAMs are formed from *n*-hexadecane thiol). The contact area of the junction is $a = 0.5$ mm^2.

In our experiments, a computer-controlled bipotentiostat held the top and bottom drops at potentials V_s and V_d relative to the reference electrode: V_s corresponds to a source voltage and V_d to a drain voltage. V_d was fixed at an oxidizing potential and V_s was ramped from an oxidizing to a reducing potential. We observed the step-like increases in the current through the junctions shown in Fig. 10. The steps occurred as V_s crossed reduction potentials of the redox species $Ru(NH_3)_6^{3+}$: −193 mV vs. Ag/AgCl (Fig. 10(a)); TCNQ: −110 mV and −660 mV vs. $Ag/AgNO_3$ (Fig. 10(b)). After the step, the current did not show any decreasing for more than 10 min.

To interpret these results, we considered a redox cycling mechanism (Fig. 11). Pickup and Murray [100], Bard et al. [101,102], and other authors [103], have observed redox cycling in electrochemical cells with two working electrodes separated by a narrow gap (15 nm–5 μm): redox molecules undergo alternate reduction on one electrode and oxidation on the other. For parallel planar electrodes of area *a*, separated by a distance

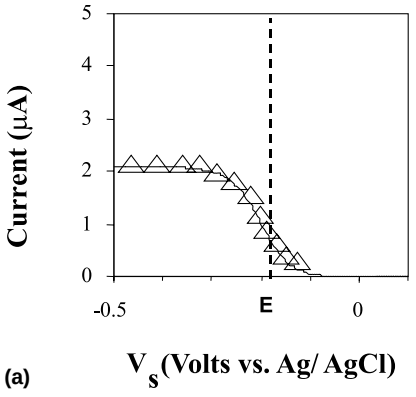

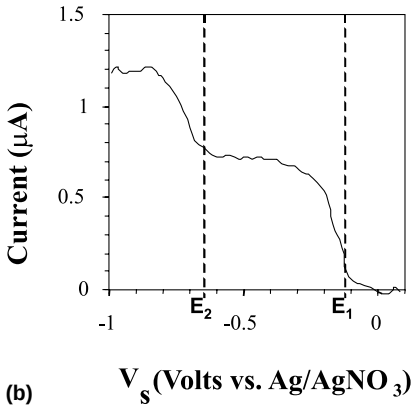

Fig. 10. (a) Current–voltage characteristics of $J_{Hg\text{–}SAM//R//SAM\text{–}Hg}$, where $R = Ru(NH_3)_6Cl_3$, at $V_d = 100$ mV vs. Ag/AgCl. V_s was swept from +100 mV to −500 mV at 50 mV/s. The line is the experimental result, and symbols △ are the data calculated from Eq. (4). (b) Current–voltage characteristics of $J_{Hg\text{–}SAM//R//SAM\text{–}Hg}$, where R = TCNQ, at $V_d = 0$ mV vs. $Ag/AgNO_3$. V_s was swept from +100 mV to −1000 mV at 50 mV/s.

d, in a solution of redox species with concentration C and diffusion constant D, the diffusion-limited redox cycling current I is given by Eq. (4), where F is Faraday's constant [104]. The current

$$I = aCFD/d \tag{4}$$

flows only when the reduction potential of the redox species falls between the potentials on the two electrodes. Bard and Wrighton [101] showed that the diffusion-limited redox cycling currents are inversely proportional to the interelectrode distance, and the current is therefore limited by the

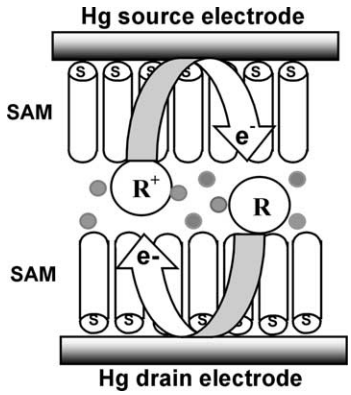

Fig. 11. Schematic representation of the cycling of the redox centers trapped between Hg electrodes supporting $-COO^-$ terminating SAMs. The arrows represent the electron-transfer processes from the electrodes to the redox site through the SAMs.

time required for redox molecules to diffuse from one electrode to the other.

Fig. 10(a) shows the fitting of the experimental values of the current to a redox-cycling mechanism for $a = 0.5$ mm^2, $Ru(NH_3)_6^{3+}] = 0.4$ mM, $d = 5$ nm, $D = 5 \times 10^{-10}$ m^2/s.

These preliminary results are compatible with the hypothesis that the molecules trapped in $J_{Hg\text{–}SAM/R/SAM\text{–}Hg}$ are confined between two electrodes separated by few nanometers, and conduct current through a redox cycling mechanism.

5. Conclusions

The junctions Hg–SAM//SAM–Hg, Hg–SAM//SAM–Metal, Hg–SAM//R//SAM–Hg are the basis for a new, physical-organic-based approach to the study of electron transport in organic nm-thick films. These systems and junctions have advantages and disadvantages relative to other systems for studying electron transport (Table 2).

The Hg-based electrode is crucial to these systems: it allows conformal (or near conformal) contact with one electrode to the other, and is therefore the basis for ease of assembly. It is, however, unclear whether the use of a liquid surface causes defects or reconstruction of the SAMs formed on it under electrostatic pressure. While

Table 2
Advantages and disadvantages of Hg-based junctions

Advantages	Disadvantages
Easy to assemble; requires relatively inexpensive equipment	Does not give single-molecule resolution
Allows exploration of electrical properties of a wide ranges of organic/organometallic functionality	Not practical for devices
Currents are averaged over a large number (10^8) of sites	Hg presents potential problems: high vapor pressure, electromigration, changes in shape under applied potential, lateral movements of SAMs
Organic components are structurally well-defined (and often oriented)	Best assembled in contact with liquid (higher reproducibility)
Can generate 10–100 s of replicate experiments, and give statistically significant data	

such effects do not seem prominent for Hg–SAM// SAM–Metal system [27–29,45] they can be important for the Hg–SAM//SAM–Hg junction, as emphasized by Majda and Slowinski [34]. The fact that the systems are more reproducible when assembled under a solvent containing alkanethiol suggests some damage to the SAM covering the Hg drop on assembly.

An unsolved problem with these junctions concerns the nature of the interface between two SAMs: this interface is still incompletely defined. Capacitance studies indicated that the junctions involving CH_3-terminated SAMs do not include polar solvent molecules. In the inclusion junctions, Hg–SAM//R//SAM–Hg – junctions involving $-COO^-$ terminated SAMs and water as solvents – the results indicate that there is electrical contact between the external working/reference electrodes and the redox site R, and suggest a thin electrolyte layer at the interface. For non-polar surfaces in contact with non-polar liquids, it appears that the junction may have included solvent when first assembled, but probably does not have included solvent after the junction has been subjected to an applied voltage (and, thus, substantial hydrostatic pressure). This inference is compatible with the idea that the hydrostatic pressure squeezes liquid from the interface of the junction. It is also compatible with Majda's suggestion that pressure on the SAMs in $J_{Hg–SAM//SAM–Hg}$, may thin them by lateral motion. It therefore appears (not surprisingly) that the inclusion or exclusion of solvent from the interface probably depends on the SAM, the solvent, and the applied potential.

Table 3 summarizes a critical comparison of the performances of these junctions. It is evident that (i) $J_{Hg–SAM//SAM–Hg}$ suffers from severe limitations when the objective of the experiments is comparison of the electrical behavior of different organic molecules. It is, however, an interesting and practical system with which to study phenomena related to inclusion of redox sites confined in a nanometer-sized volume; (ii) $J_{Hg–SAM//SAM–Au(Ag)}$ junction represents a useful workhorse for molecular electronics.

The results obtained with these Hg–SAM based junctions provide a new experimental approach to the measurement and comparison of electron-transport rates (i) across a large variety of organic and organometallic thin films, (ii) across different kinds of chemical bonds, and (iii) across nm-scale gaps in processes mediated by redox molecules as electron carriers. The results we have obtained in all of the systems examined to date indicate that the mechanism of electron transport is tunneling between the metal junctions across the SAMs. Although, when using these systems, we always measure a finite current for non-zero voltage, we again emphasize that these organic and organometallic monolayers are electrically "conducting" only in the sense that they support tunneling better than vacuum does. There is no analogy between "conductivity" in these molecular films and conductivity in copper films: one involves tunneling, and the other transport of conduction-band electrons. The only circumstance in which we might hope to see Ohmic conduction through molecules would be one in which the Fermi level of the

Table 3
Comparison of the performances of the Hg-based junctions

Junction	Advantages	Disadvantages
$J_{Hg-SAM//SAM-Hg}$	Easy to assemble	Interdigitation and lateral spreading of facing SAMs at high voltage
	Common metals for both electrodes	Difficult to characterize the SAMs on Hg
	Both electrodes are compliant	Difficult to measure contact area
		Requires assembly in liquid
$J_{Hg-SAM//SAM-Au(Ag)}$	Easy to assemble	
	SAMs on metals (Au/Ag/Pd) can be prepared/characterized independently	Requires assembly in liquid
	Generates statistically significant number of measurements	
	Easy to measure the contact area	
$J_{Hg-SAM//R//SAM-Hg}$	Easy to assemble	Uncertainty about structure at the interface, solvent included, and details of the mechanism of electron transport
	Possible inclusion of a variety of redox centers	Requires external electrodes to control the Fermi level of the two electrodes

electrodes were brought into resonance with the energy of the molecular HOMO/LUMO orbitals [4,105].

An important result of these studies is the finding that the values of the attenuation factor β for aliphatic chains ($\beta = 0.87 \pm 1\ \mathring{A}^{-1}$) and polyphenylene chains ($\beta = 0.61 \pm \mathring{A}^{-1}$) are similar to those found for soluble structures D–B–A, where the tunneling mechanism is well-established. These similarities suggest that theories for interpreting electron transfer in molecular systems may be applicable to electron transport in mesoscopic systems [106]. In the theory describing non-adiabatic electron transfer in molecular systems, the rate of electron transfer (k_{ET}) is given by Eq. (5) [107–110]; this equation explicitly separates contributions from the electronic and nuclear wavefunctions. Here, H_{DA} describes the electronic coupling between the electronic wavefunctions of the donor (D) and the acceptor (A), and FCWD is the Frank–Condon weighted density of states that describes the overlap of nuclear wavefunctions of the reactant and the product [111]:

$$k_{ET} = 4\pi/hH_{DA}^2\mathrm{FCWD}, \tag{5}$$

$$k_{ET} \propto H_{DA}^2 \propto \exp(-\beta d). \tag{6}$$

H_{DA} (and therefore k_{ET}) depends exponentially on the distance separating the electron donor and the electron acceptor, because of the exponential drop-off of the electronic wavefunctions with distance (Eq. (6)). Several strategies have been employed to calculate H_{DA} for D–B–A assemblies [112–114]. These approaches build on the application of superexchange used by McConnell [115], which assumes that indirect coupling between D and A takes place by mixing between states on D and A and high energy states on the bridging group. Bardeens's analysis of tunneling [116] and Landauer's scattering formalism [117,118] have been used recently [88,119,120] to develop models for electron transport across molecules in MIM junctions. This approach relates the conductance (g) to the transmission function T from one contact to another (Eqs. (7) and (8)) [106,120]. In these equations L is the length of the molecule and h is Planck's constant. There is an

$$g \propto (e^2/h)T^2, \tag{7}$$

$$T \approx e^{-(2mEg)^{1/2}L/h} \tag{8}$$

analogy between the transmission function T in Eq. (7) and the electronic-coupling factor H_{DA} in Eq. (5); the dependence of both H_{DA} and T on the

length of the molecule is exponential. As with calculations of H_{DA}, different methods have been used to calculate T [106]. Eqs. (5) and (7) indicate that both the rate of electron transfer, and the conductance through a molecular wire depend on electronic coupling between the initial and final states [89,121].

We believe that the results obtained in this work indicate that these junctions are systems that can be used to collect reliable experimental data on the electrical behavior of a wide variety of molecular systems. They represent a useful complement to physics-based experimental methods. We hope that they will contribute to the understanding of electron transport in mesoscale systems, and to the design of molecular electronic devices.

6. Note added in proof

Porter (J.D. Porter, A.S. Zimm, J. Phys. Chem. 97 (1993) 1190) made early measurements of tunneling between two mercury drops through water.

Acknowledgements

This work was supported by the ONR, DARPA, and the NSF (ECS-9729405)(USA) and by the CNR (Italy). We are grateful to M.A. Ratner (Nothwestern University), V. Mujica (Universidade Central de Venezuela) to C.D. Frisbie (University of Minnesota) for fundamental discussions, and to M. Majda and K. Slowinski (University of California), R. Shashidhar (Naval Research Laboratories, Washinghton) for exchanging comments and suggestions. The authors thank A.E. Cohen, R. Haag, R.E. Holmlin, R.F. Ismagilov, and A. Terford for their contributions to the work.

References

[1] V. Balzani (Ed.), Electron Transfer in Chemistry, vols. I–V, Wiley, Weinheim, 2001.
[2] B. Mann, H. Kuhn, J. Appl. Phys. 42 (1971) 4398.
[3] A. Aviram, M.A. Ratner, Chem. Phys. Lett. 29 (1974) 277.
[4] H.D. Sikes, J.F. Smalley, S.P. Dudek, A.R. Cook, M.D. Newton, C.E.D. Chidsey, S.W. Feldberg, Science 291 (2001) 1519.
[5] E.P.A.M. Bakker, A.L. Roest, A.W. Marsman, L.W. Jenneskens, L.I. De Jong-van Steensel, J.J. Kelly, D. Vanmaekelberg, J. Phys. Chem. B 104 (2000) 7266.
[6] S. Creager, C.J. Yu, C. Bamdad, S. O'Connor, T. MacLean, E. Lam, Y. Chong, G.T. Olsen, J. Luo, M. Gozin, J.F. Kayyem, J. Am. Chem. Soc. 121 (1999) 1056.
[7] S.B. Sachs, S.P. Dudeek, R.P. Hsung, L.R. Sita, J.F. Smalley, M.D. Newton, S.W. Feldberg, C.E.D. Chidsey, J. Am. Chem. Soc. 119 (1997) 10563.
[8] K. Slowiski, R.V. Chamberlain, C.J. Miller, M. Majda, J. Am. Chem. Soc. 119 (1997) 11910.
[9] K. Weber, L. Hockett, S. Creager, J. Phys. Chem. B 101 (1997) 8286.
[10] H.O. Finklea, D. Hanshew, J. Am. Chem. Soc. 114 (1992) 3173.
[11] J.F. Smalley, S.W. Feldberg, C.E.D. Chidsey, M.R. Lindford, M. Newton, Y.-P. Liu, J. Phys. Chem. 99 (1995) 13141.
[12] A.M. Becka, C.J. Miller, J. Phys. Chem. 96 (1992) 2657.
[13] C.E.D. Chidsey, Science 251 (1991) 919.
[14] Y. Xia, J.A. Rogers, K.E. Paul, G.M. Whitesides, Chem. Rev. 99 (1999) 1823.
[15] R. Weisendanger, Scanning Probe Microscopy and Spectroscopy, Cambridge University Press, Cambridge, 1994.
[16] A. Ulman, Chem. Rev. 96 (1996) 1533.
[17] S. Ranganathan et al. (submitted).
[18] J.H. Schön, H. Meng, Z. Bao, Nature 413 (2001) 713.
[19] J.H. Schön, H. Meng, Z. Bao, Nature 294 (2001) 2138.
[20] F.F. Fan, J.G. Yang, S.M. Dirk, D.W. Price, D. Kosynkin, J.M. Tour, A.J. Bard, J. Am. Chem. Soc. 213 (2001) 2454.
[21] R.M. Metzger, T. Xu, I. Petersen, J. Phys. Chem. 105 (2001) 7280.
[22] M.A. Reed, J. Chen, A.M. Rawlett, D.W. Price, J.M. Tour, Appl. Phys. Lett. 78 (2001) 3735.
[23] Z.J. Donhauser, B.A. Mantooth, K.F. Kelly, L.A. Bumm, J.D. Monnell, J.J. Stapleton, D.W. Price Jr., A.M. Rawlett, D.L. Allara, J.M. Tour, P.S. Weiss, Science 292 (2001) 2303.
[24] X.D. Cui, A. Primak, X. Zarate, J. Tomfohr, O.F. Sankey, A.L. Moore, T.A. Moore, D. Gust, G. Harris, S.M. Lindsay, Science 294 (2001) 571.
[25] H.J. Park, A.K.L. Lim, E.H. Anderson, A.P. Alivisatos, P.L. McEuen, Nature 407 (2000) 680.
[26] A.E. Cohen, R.F. Ismagilov, M.A. Rampi, G.M. Whitesides (in preparation).
[27] M.L. Chabinyc, X. Chen, R.E. Holmlin, H. Jacobs, H. Skulason, C.D. Frisbie, V. Mujica, M.A. Ratner, M.A. Rampi, G.M. Whitesides (submitted).
[28] R.E. Holmlin, R. Haag, R.F. Ismagilov, M.A. Rampi, G.M. Whitesides, J. Am. Chem. Soc. 123 (2001) 5075.
[29] R.E. Holmlin, R. Haag, R.F. Ismagilov, V. Mujica, M.A. Ratner, M.A. Rampi, G.M. Whitesides, Angew. Chem. Int. Engl. Ed. 40 (2001) 2316.

[30] D.J. Wold, C.D. Frisbie, J. Am. Chem. Soc. 123 (2001) 5549.
[31] C.P. Collier, E.W. Wong, M. Beloradsky, F.M. Raymo, J.F. Stoddard, P.J.R.S. Williams, J.R. Heath, Science 280 (2000) 1172.
[32] J. Collet, S. Lenfant, D. Vuillaume, O. Bouloussa, F. Rondelez, J.M. Gay, K. Kham, C. Chevrot, Appl. Phys. Lett. 76 (2000) 1339.
[33] D.J. Wold, C.D. Frisbie, J. Am. Chem. Soc. 122 (2000) 2970.
[34] K. Slowinski, M. Majda, J. Electroanal. Chem. 491 (2000) 13.
[35] R.M. Metzger, Acc. Chem. Res. 32 (1999) 950.
[36] J.K. Gimzewski, C. Joachim, Science 283 (1999) 1683.
[37] V.J. Langlais, R.R. Schittler, H. Tang, A. Gourdon, C. Joachim, J. Gimzewski, Phys. Rev. Lett. 83 (1999) 2809.
[38] J. Chen, M.A. Reed, A.M. Rawlett, J.M. Tour, Science 286 (1999) 1550.
[39] C. Zhou, M.R. Despande, M.A. Reed, L. Jones II, J.M. Tour, Appl. Phys. Lett. 71 (1997) 611.
[40] C. Kergueris, J.P. Bourgoin, S. Palacin, D. Esteve, C. Urbina, M. Magoga, C. Joachim, Phys. Rev. B 59 (1999) 12505.
[41] L.A. Bumm, J.J. Arnold, T.D. Dunbar, D.L. Allara, P.S. Weiss, J. Phys. Chem. B 103 (1999) 8122.
[42] Y. Xue, S. Datta, S. Hong, R. Reifenberg, J.I. Henderson, C.P. Kubiak, Phys. Rev. B 59 (1999) R7852.
[43] K. Slowinski, H.K.Y. Fong, M. Majda, J. Am. Chem. Soc. 103 (1999) 7257.
[44] J. Chen, L.C. Calvet, M.A. Reed, D.W. Carr, D.S. Grubisha, D.W. Bennet, Chem. Phys. Lett. 331 (1999) 741.
[45] R. Haag, M.A. Rampi, R.E. Holmlin, G.M. Whitesides, J. Am. Chem. Soc. 103 (1999) 7895.
[46] W. Tian, S. Datta, S. Hong, R. Reifenberger, J. Henderson, C. Kubiak, J. Chem. Phys. 109 (1998) 2874.
[47] P.S. Weiss, L.A. Bumm, T.D. Dunbar, T.P. Burgin, J.M. Tour, D.L. Allara, Ann. N. Y. Acad. Sci. 852 (1998) 145.
[48] M.A. Rampi, O.J. Schueller, G.M. Whitesides, Appl. Phys. Lett. 72 (1998) 1781.
[49] D. Poraths, A. Bezryadin, S. De Vries, C. Dekker, Nature 403 (2000) 635.
[50] C. Joachim, J.K. Gimzewski, Chem. Phys. Lett. 265 (1997) 353.
[51] M.A. Reed, C. Zhou, C.J. Muller, T.P. Burgin, J.M. Tour, Science 278 (1997) 252.
[52] A.-A. Dhirani, P.H. Lin, P. Guyot-Sionnest, R.W. Zehner, L.R. Sita, J. Chem. Phys. 106 (1997) 5249.
[53] A. Bezryadin, C. Dekker, J. Vac. Sci. Technol. A 15 (1997) 793.
[54] R.P. Andres, J.D. Bielefeld, J.I. Henderson, D.B. Janes, V.R. Kolagunta, C.P. Kubiak, W. Mahoney, R.G. Osifchin, Science 273 (1996) 1690.
[55] L.A. Bumm, J.J. Arnold, M.T. Cygan, T.D. Dunbar, T.P. Burgin, L. Jones, D.L. Allara, J.M. Tour, P.S. Weiss, Science 271 (1996) 1705.
[56] C. Joachim, J.K. Gimzewski, R.R. Schlitter, C. Chavy, Phys. Rev. Lett. 74 (1995) 2102.
[57] S. Datta, D.B. Janes, R.P. Andres, C.P. Kubiac, R.G. Reifenberg, Semicond. Sci. Technol. 13 (1998) 1347.
[58] C. Joachim, J.K. Gimzewski, A. Aviram, Nature 408 (2000) 541.
[59] J.C. Ellenbogen, J.C. Love, IEEE 88 (2000) 386.
[60] M. Magoga, C. Joachim, Phys. Rev. B 59 (1999) 16011.
[61] M.A. Reed, J.M. Tour, Sci. Am. 282 (2000) 86.
[62] V. Mujica, M. Kemp, A. Roitberg, M.A. Ratner, J. Chem. Phys. 104 (1996) 7296.
[63] J.M. Seminario, C.E. De La Cruz, P.A. Derosa, J. Am. Chem. Soc. 123 (2001) 5616.
[64] O.M. Magnussen, B.M. Ocko, M. Deutsch, M.J. Regan, P.S. Pershan, L.E. Berman, D. Abernathy, J.F. Legrand, G. Grubel, Nature 384 (1996) 250.
[65] A. Demoz, D.J. Harrison, Langmuir 9 (1993) 1046.
[66] C. Bruckner-Lea, R.J. Kimmel, J. Janata, J.F.T. Conroy, K. Caldwell, Electrochim. Acta 40 (1995) 2897.
[67] K. Slowinski, R.V. Chamberlain II, R. Bilewicz, M. Majda, J. Am. Chem. Soc. 118 (1996) 4709.
[68] J.N. Israelachvili, Intramolecular and Surface Forces, Academic Press, New York, 1992.
[69] U. Raviv, P. Laurat, J. Klein, Nature 413 (2001) 51.
[70] J. Gao, W.D. Luedtke, U. Landman, Phys. Rev. Lett. 79 (1997) 705.
[71] P.E. Laibinis, B.J. Palmer, S.W. Lee, G.K. Jennigs, Thin Solid Films 24 (1998) 1.
[72] S. Frey, V. Stadler, K. Heister, W. Eck, M. Zharnikov, M. Grunze, B. Zeysing, A. Terfort, Langmuir 17 (2001) 2408.
[73] M.N. Paddon-Row, in: V. Balzani (Ed.), Electron Transfer in Chemistry, vol. III, Wiley-VCH, Weinheim, 2001, p. 179.
[74] D. Guest, T.M. Moore, A.L. Moore, in: V. Balzani (Ed.), Electron Transfer in Chemistry, vol. III, Wiley-VCH, Weinheim, 2001, p. 272.
[75] F. Scandola, C. Chorboli, M.T. Indelli, M.A. Rampi, in: V. Balzani (Ed.), Electron Transfer in Chemistry, vol. 3, Wiley-VCH, Weinheim, 2001, p. 337.
[76] J.W. Verhoeven, J. Kroon, M.N. Paddon-Row, A.M. Oliver, in: D.O. Hall, G. Grassi (Eds.), Photoconversion Processes For Energy and Chemicals, Elsevier, Amsterdam, 1989, p. 100H.D.
[77] M.N. Paddon-Row, Acc. Chem. Res. 27 (1994) 18.
[78] A. Helms, D. Heiler, G. McLendon, J. Am. Chem. Soc. 114 (1992) 6227.
[79] L. De Cola, S. Walter, P. Belser, R. Wiliams J. Am. Chem. Soc. (submitted).
[80] A. Ponce, H.B. Gray, J.R. Winkler, J. Am. Chem. Soc. 122 (2000) 8187.
[81] E. Babini, I. Bertini, M. Borsari, F. Capozzi, C. Luchinat, X. Zhang, G.L.C. Moura, I.V. Kurnikov, D.N. Beratan, A. Ponce, J.A. Di Bilio, J.R. Winkler, H.B. Gray, J. Am. Chem. Soc. 122 (2000) 4532.
[82] C.C. Page, C. C Moser, X. Chen, P.L. Dutton, Nature 47 (1999) 52.
[83] S.O. Kelley, J.K. Barton, Science 283 (1999) 375.
[84] B. Giese, M. Spichty, S. Wessely, Pure Appl. Chem. 75 (2001) 449.

[85] B. Giese, J. Amaudrut, A.K. Köhler, M. Spormann, S. Wessely, Nature 412 (2001) 318.
[86] D.V. Wold, R. Haag, M.A. Rampi, C.D. Frisbie, J. Phys. Chem. B 106 (2002) 2813.
[87] V. Mujica, A. Roitberg, M.A. Ratner, J. Chem. Phys. 112 (2000) 6934.
[88] V. Mujica, A.E. Roitberg, M.A. Ratner, J. Chem. Phys. 112 (2000) 6834.
[89] D. Segal, A. Nitzan, M.A. Ratner, W.B. Davis, J. Phys. Chem. 104 (2000) 2790.
[90] M. Fujihira, H. Inokuchi, Chem. Phys. Lett. 17 (1972) 554.
[91] L. Salem, Molecular Orbital Theory of Conjugated Systems, Benjamin, New York, 1966.
[92] C.A. Naleway, L.A. Curtiss, J.R. Miller, J. Chem. Phys. 95 (1991) 8434.
[93] H.B. Gray, J.R. Winkler, Annu. Rev. Biochem. 65 (1996) 537.
[94] N. Beratan, J.N. Betts, J.N. Onuchic, Science 252 (1991) 1285.
[95] J.L. Sessler, M. Sathiosatham, C.T. Brown, T.A. Rhodes, G.B. Wiederrecht, J. Am. Chem. Soc. 123 (2001) 3655.
[96] J.A. Roberts, J.P. Kirby, D.G. Nocera, J. Am. Chem. Soc. 119 (1997) 9230.
[97] P.J.F. DeRedge, S.A. Williams, M.J. Therien, Science 269 (1995) 1409.
[98] L. Yan, C. Marzolin, A. Terfort, G.M. Whitesides, Langmuir 13 (1997) 6704.
[99] A. Soudackov, S. Hammes-Schiffer, J. Am. Chem. Soc. 121 (1999) 10598.
[100] P.G. Pickup, R.W. Murray, J. Am. Chem. Soc. 105 (1983) 4510.
[101] A.J. Bard, J.A. Crayston, G.P. Kittlesen, T. Varco Sea, M.S. Wrighton, Anal. Chem. 58 (1986) 2321.
[102] F.F. Fan, J. Kwak, A.J. Bard, J. Am. Chem. Soc. 118 (1996) 9669.
[103] A.E. Cohen, R.R. Kunz, Sens. Actuator B – Chem. 62 (2000) 23.
[104] A.J. Bard, Electrochemical Methods: Fundamentals and Applications, Wiley, New York, 1980.
[105] W.B. Davis, W.A. Svec, M.A. Ratner, M.R. Wasielewski, Nature 396 (1998) 60.
[106] S. Datta, Electronic Transport in Mesoscopic Systems, Cambridge University Press, Cambridge, 1995.
[107] R.A. Marcus, N. Sutin, Biochim. Biophys. Acta 811 (1985) 265.
[108] P.F. Barbara, T.J. Meyer, M.A. Ratner, J. Phys. Chem. 100 (1996) 13148.
[109] N.S. Hush, Coord. Chem. Rev. 64 (1985) 135.
[110] M.D. Newton, Chem. Rev. 91 (1991) 767.
[111] R.A. Marcus, J. Chem. Phys. 24 (1956) 966.
[112] M. Bixon, J. Jortner, Adv. Chem. Phys. 106 (1999) 35.
[113] M. Kuznetov, J. Ulstrup, A.M.K. Sov, Electron Transfer in Chemistry and Biology: An Introduction to the The Theory, Wiley, New York, 1995.
[114] C. Liang, M.D. Newton, J. Phys. Chem. 96 (1992) 2855.
[115] H.M. McConnell, J. Chem. Phys. 35 (1961) 508.
[116] J. Bardeen, Phys. Today 22 (1969) 40, and references therein.
[117] R. Landauer, Phys. Lett. A 8 (1981) 91, and references therein.
[118] Y. Imry, R. Landauer, Rev. Mod. Phys. 71 (1999) S306.
[119] M.A. Ratner, B. Davis, M. Kemp, V. Mujica, A. Roitberg, S. Yaliraki, Ann. N. Y. Acad. Sci. 852 (1998) 22.
[120] E.G. Emberly, G. Kirczenov, Phys. Rev. B 61 (2000) 5740.
[121] A. Nitzan, J. Phys. Chem. A 105 (2001) 2677.